

## Retraction

# Retracted: Application of Machine Learning in Multi-Directional Model to Follow Solar Energy Using Photo Sensor Matrix

### International Journal of Photoenergy

Received 15 August 2023; Accepted 15 August 2023; Published 16 August 2023

Copyright © 2023 International Journal of Photoenergy. This is an open access article distributed under the Creative Commons Attribution License, which permits unrestricted use, distribution, and reproduction in any medium, provided the original work is properly cited.

This article has been retracted by Hindawi following an investigation undertaken by the publisher [1]. This investigation has uncovered evidence of one or more of the following indicators of systematic manipulation of the publication process:

- (1) Discrepancies in scope
- (2) Discrepancies in the description of the research reported
- (3) Discrepancies between the availability of data and the research described
- (4) Inappropriate citations
- (5) Incoherent, meaningless and/or irrelevant content included in the article
- (6) Peer-review manipulation

The presence of these indicators undermines our confidence in the integrity of the article's content and we cannot, therefore, vouch for its reliability. Please note that this notice is intended solely to alert readers that the content of this article is unreliable. We have not investigated whether authors were aware of or involved in the systematic manipulation of the publication process.

Wiley and Hindawi regrets that the usual quality checks did not identify these issues before publication and have since put additional measures in place to safeguard research integrity.

We wish to credit our own Research Integrity and Research Publishing teams and anonymous and named external researchers and research integrity experts for contributing to this investigation.

The corresponding author, as the representative of all authors, has been given the opportunity to register their agreement or disagreement to this retraction. We have kept a record of any response received.

### References

- [1] P. Dhanalakshmi, V. Venkatesh, P. S. Ranjit et al., "Application of Machine Learning in Multi-Directional Model to Follow Solar Energy Using Photo Sensor Matrix," *International Journal of Photoenergy*, vol. 2022, Article ID 5756610, 9 pages, 2022.

## Research Article

# Application of Machine Learning in Multi-Directional Model to Follow Solar Energy Using Photo Sensor Matrix

**P. Dhanalakshmi,<sup>1</sup> V. Venkatesh,<sup>2</sup> P. S. Ranjit,<sup>3</sup> N. Hemalatha,<sup>4</sup> S. Divyapriya,<sup>5</sup> R. Sandhiya,<sup>6</sup> Sumit Kushwaha,<sup>7</sup> Asmita Marathe,<sup>8</sup> and Mekete Asmare Huluka<sup>9</sup>**

<sup>1</sup>Department of Computer Science and Systems Engineering, Sree Vidyanikethan Engineering College (SVEC), Tirupati, Andhra Pradesh 517102, India

<sup>2</sup>Department of Electrical and Electronics Engineering, Rajalakshmi Engineering College, Chennai, Tamil Nadu 602105, India

<sup>3</sup>Department of Mechanical Engineering, Aditya Engineering College, Surampalem, Andhra Pradesh 533437, India

<sup>4</sup>Institute of Electronics and Communication Engineering, Saveetha School of Engineering (SIMATS), Chennai, Tamil Nadu 600124, India

<sup>5</sup>Department of Electrical and Electronics Engineering, Karpagam Academy of Higher Education, Eachanari, Tamil Nadu 641021, India

<sup>6</sup>Department of Computer Science Engineering, RMK College of Engineering and Technology (RMKCET), Thiruvallur, Tamil Nadu 601206, India

<sup>7</sup>Department of Computer Applications, University Institute of Computing, Chandigarh University, Punjab 140413, India

<sup>8</sup>Department of Technology, Savitribai Phule Pune University, Pune, Maharashtra 411007, India

<sup>9</sup>Department of Electrical and Computer Engineering, Institute of Technology, University of Gondar, Gondar, Ethiopia

Correspondence should be addressed to Mekete Asmare Huluka; mekete.asmare@uog.edu.et

Received 19 July 2022; Revised 13 September 2022; Accepted 19 September 2022; Published 14 October 2022

Academic Editor: BR Ramesh Babu

Copyright © 2022 P. Dhanalakshmi et al. This is an open access article distributed under the Creative Commons Attribution License, which permits unrestricted use, distribution, and reproduction in any medium, provided the original work is properly cited.

In this paper, we introduce a deep neural network (DNN) for forecasting the intra-day solar irradiance, photovoltaic PV plants, regardless of whether or not they have energy storage, can benefit from the work being done here. The proposed DNN utilises a number of different methodologies, two of which are cloud motion analysis and machine learning, in order to make forecasts regarding the climatological conditions of the future. In addition to this, the accuracy of the model was evaluated in light of the data sources that were easily accessible. In general, four different cases have been investigated. According to the findings, the DNN is capable of making more accurate and reliable predictions of the incoming solar irradiance than the persistent algorithm. This is the case across the board. Even without any actual data, the proposed model is considered to be state-of-the-art because it outperforms the current NWP forecasts for the same time horizon as those forecasts. When making predictions for the short term, using actual data to reduce the margin of error can be helpful. When making predictions for the long term, however, weather information can be beneficial.

## 1. Introduction

Researchers in the field of meteorology have been interested in solar radiation for centuries. Irradiance forecasting has produced precise and accurate results in a number of recently conducted studies as a result of a variety of recently developed technologies [1]. PV is a technology that has been steadily increasing its share in the global power generation

industry, which has made it a key player in the global energy market. This industry has experienced consistent growth over the past ten to twelve years, with more than one hundred gigawatts of new grid-connected capacity being added in just the year 2018 [2]. As a consequence of this, a significant number of PV deployments that are currently taking place and those that are anticipated to take place in the near future imply significant levels of PV penetration

in a variety of power systems. Power can be obtained directly from the sun. But it can get little power when it is surrounded by rain. Solar energy is used all over the world. Also, the use of solar energy to generate electricity or heat and convert seawater into fresh water is becoming increasingly popular. Because of the inherently intermittent nature of PV production, for instance, the casuistic threat to the grid stability that is posed by passing clouds is made significantly worse. PV power plants are unable to provide accurate forecasts regarding their future output, which makes it difficult for grid operators and PV owners to manage the system and sell their output on the market for electricity. As a consequence of these constraints, multiple photovoltaic (PV) plants located in different parts of the country have traditionally been combined [3]. More recently, however, a variety of energy storage systems, primarily batteries, have been installed in close proximity to PV plants [4]. PV plants are subject to significant costs in the form of batteries, which are prone to experiencing accelerated wear and tear in the event that operating conditions are not properly monitored [5].

In this setting, the capacity to accurately forecast irradiance and, as a consequence, PV output is absolutely necessary. Irradiance forecasting improves the reliability of operation of photovoltaic (PV) systems, also known as dispatch ability [6]. The integration of batteries into photovoltaic plants makes it possible to use smaller batteries, which is necessary for hybrid power plants to be able to operate reliably on the electricity market [7]. By using the forecast, it is also possible to optimise the operation of the plant, obtain information about future production, and, as a result, reduce the ageing of the batteries. Solar cells, also known as photovoltaics, are electronic devices that convert sunlight directly into electricity. Modern solar cells, as most people recognize them today, are found in panels mounted on homes and computers. Solar cells are currently one of the fastest growing renewable energy technologies and are poised to play a massive role in the future global electricity generation mix. There are a variety of approaches that can be taken to forecast the activity of the sun. There are two different strategies to choose from: physical and data-driven [8]. While data-driven approaches make primary use of historical data as their primary input for prediction, physical approaches rely on the knowledge that is derived from atmospheric science [9]. In order to choose an approach that is appropriate, you need to take into account the target forecasting horizon as well as the time-step, also known as the granularity. Both of these factors are determined by the anticipated use of the forecast [10]. The forecasts for the following day are the primary focus of this research (with a horizon of up to 6h ahead) [11–14]. The use of numerical weather predictions is favoured for longer-term forecasts, while time series and sky images are preferred for more immediate forecasts [14]. Solar cells can be combined to supply electricity on a commercial basis or to connect electricity to small grids or to obtain electricity for personal use. Using solar cells is the best way to provide electricity to people living outside the grid. The cost of manufacturing panels equipped with solar cells has fallen

dramatically over the past decades. For this reason it has become a viable form of electricity to use. Solar panels have a lifespan of about 25 years and come in different colours based on the materials used in manufacturing.

An artificial neural network, or ANN, is one that simulates the human brain natural capacity to recognise and remember certain patterns [15]. It is concluded in both of these reviews that these methods produce accurate forecast results. However, it is difficult to make direct comparisons between them because each forecast is based on a unique set of circumstances and geographic locations. When reviewing the most recent research on solar forecasting, comparability and reproducibility issues frequently arise in the literature. In order to avoid this, the ROPES guidelines for solar forecasting that are proposed in this document will be followed [16]. The authors in [17] provides a classification system for the various methods of weather forecasting based on the length of their forecasting horizons and the climatology of the local area. The RRMSE of the different methods ranges from 20% to 40% for temperate climate and intra-day forecasts, with the best performance coming from machine learning and cloud motion methods. For forecasts made one hour in the future using machine learning methods such as those described in [18], the error rate ranges between 20 and 25%. Cloud motion approaches have errors of approximately 28% and 10%, respectively, for one-hour forecasts. When applied to forecasting horizons of one hour and six hours, this method produces error rates of 22.6 and 32.1%, respectively. Concentrated solar power (CSP) uses mirrors to concentrate the sun's rays. These rays heat the liquid. This heated liquid flows through the heat exchanger to form steam. The steam rotates the turbine to generate electricity. Concentrated solar energy is used to generate electricity in large-scale power plants.

Satellite images and real-time irradiance measurements are used as inputs to the forecast models in almost all of these studies. The forecast model must figure out how the weather will change over time, in addition to figuring out how to compute the irradiance from satellite images, in the case of the former. Both of these tasks are burdensome. In order to accomplish this, it is necessary to rely on data that is frequently unreliable or that is simply unavailable. A few examples of the types of installations that fall into this category include those that are small, have constrained budgets, are located in inaccessible areas, or have facilities that are difficult to maintain data acquisition systems. Other works in the corpus of research have attempted to address these limitations [19] developed a method for predicting irradiance that did not require the use of real-time measurements. This method relied on satellite images and a technique known as support vector regression (SVR). However, the SVR model must still be validated against the data that was collected. A concentrated solar power plant usually consists of a block of generators. These direct the sun's rays to a tall and condensing tower. One of the main advantages of such plants over power plants with panels containing solar cells is the presence of molten salt in them. Molten salt stores heat. This makes it possible to generate electricity even a few hours after the sun goes down. These models can be

trained and deployed in areas where there is no telemetry at all by making use of data from a select number of locations. Nonetheless, despite the fact that these two works make an effort to avoid the requirement of using measured irradiance, their models must still be trained using measured data.

## 2. Related Works

Neural networks have the inherent capacity (theoretically) to model any unambiguous function, regardless of how complicated the function may be (NNs). When trying to get a grasp on what neural networks are all about, Rosenblatt perceptron is a good place to begin. In the same way that there are many inputs in the brain, each of which has a unique electrical signal, these inputs are integrated, and whether or not a neuron fires are contingent on a threshold [20]. The input and the weights are multiplied together to generate a vector inner product, which is then used to determine whether or not the neuron will fire. Each individual node has a weight vector as well as a linear transformation associated with it. After that, the input is processed by non-linearity, which produces the distinctive signal characteristics that are associated with each node. An artificial neural network (ANN) is, as its name suggests, a collection of nodes that are interconnected with one another and that are capable of being trained to carry out a particular task [21]. To know the benefits of solar energy, we need to know what it is and what types of solar energy there are. First know what it is a renewable source of energy derived from the sun can generate heat and electricity for any use. Although it is a standard source, it is important to point out that it is not without its drawback, which also affects its purpose and use. It is derived directly from radiation reaching our planet from the Sun in the form of light, heat or ultraviolet rays. Depending on how solar energy is available, there are different types.

In supervised learning, the data that is used for training has a specific format that has been determined in advance. As a consequence of this, users are aware of the expected output that the function that connects input and output should produce when it comes to making predictions (be it classification or regression). In the same way that supervised learning works, we need to find a system that can learn a functional approximation based on a predefined structure that exists between the input and the output [22]. The most basic form of neural network, also known as a shallow neural network (SNN), has just one hidden layer of nodes sitting in between the network input and output. Shallow neural networks (SNNs) are the most common form of neural network. It is only capable of learning the most fundamental functions in a reasonable timeframe. Learning at a deep level is necessary in order to master more complicated functions. Deep learning refers to the process of stacking a neural network (NN) with more than one intermediate layer. When more layers are added to a network, it shortens the amount of time needed for the network to learn more complex functions. Stacking hidden layers can be done by adding new hidden layers to an existing hidden layer [23]. As its name suggests, it is a form of renewable and clean energy that uses

the sun's energy to generate electricity. Unlike solar panels that use photoelectric energy to produce electricity from photons of light found in solar radiation, this energy uses this radiation to heat a liquid. When the sun's rays hit the liquid, it heats up, and this hot liquid can be used for various applications. To get a better idea, the energy consumption of a hospital, a hotel or a house corresponds to 20% of hot water use. With solar thermal energy we can heat water with the energy of the sun and use it so that we do not have to use fossil or other energy in this energy sector. Solar thermal energy contributes significantly to reducing energy costs, resulting in savings in energy and reducing CO<sub>2</sub> emissions that are responsible for global warming and climate change.

The number of parameters that can be learned and the efficiency with which this can be done are both determined by the connections that exist between the layers of a NN. Feed-forward neural networks make use of layers that are completely interconnected (NNs with a linear graph). Every one of the nodes in one layer is connected to every one of the nodes in the layer below it. This method begins with a linear transformation of the data and then transitions into non-linearity. This is necessary because each connection has a weight vector that corresponds to it and it presents a challenge when dealing with image data because nodes would need to be created for each individual pixel. In the case of an image with a resolution of one megabyte, for instance, each layer in an FCN would have a width of 0.106 [24].

*2.1. Convolutional Neural Networks.* There is a theory that the visual cortex of an animal functions as an intricately networked system of neurons that transmits a specific electrical signal from layer to layer, beginning with an image captured by the eye and ending with an understanding of what was captured by the brain. This theory is supported by a number of studies that have been conducted to test the hypothesis. When done in this manner, the first layer focuses on features that are considered more fundamental, such as colour gradients and lighting, before moving on to the next layer, which focuses on features that are considered more fundamental, such as textures and shadows (e.g. facial features) [25]. It uses heat thanks to solar collectors that receive the sun's rays and convert it into a working fluid. It is used to heat buildings and water, move turbines, and destroy dry grain or waste.

For instance, each layer is responsible for identifying an abstract feature, which in turn assists the subsequent layers in identifying additional abstract features. Because of this, the animal neurons are trained to respond to a variety of stimuli in a manner that is unconscious; as a result, the animal learns. This is precisely the purpose that convolution neural networks (CNNs) are meant to serve. Our artificial network is able to learn how to react to increasingly abstract features in the image data as it progresses through each successive layer. This enables the output layer to learn the geometry of a variety of different objects. However, because the network selects the abstract features it learns for each image classification task, this results in a loss of interpretability. The features, in their essence, are not something that can be written down



FIGURE 1: Proposed Model.

explicitly but are instead something that is learned by the machine through its imagination [26].

This is done rather than having every node in the subsequent layer connected to all of the other nodes in the layer below it. Due to the fact that CNNs were developed for the purpose of taking an image as their input, the linear transformation is represented by the convolution function that is present in each node. The comparison of this system to a biological network is apt. This idea is founded on the observation that the degree of correlation that exists between neighbouring pixels in an image weakens with increasing distance from the pixels that are being discussed in the image. This has the additional benefit that, instead of training a weight to be used between each pair of nodes in the convolutional network, the convolutional kernel is used for each node in the network [27]. The classification of images frequently makes use of CNNs that have multiple layers. As a direct consequence of this, the convolution function of CNNs handles shift invariance in an automatic fashion. CNNs are now programmed to learn about the geometric properties of features rather than the relative positions of pixels in images. Because the network looks for feature maps rather than particular pixel sequences, it is consequently much simpler to recognise objects in pictures as a consequence of this [28, 29].

### 3. Proposed Method

It is necessary to make a number of choices before defining the architecture of a CNN (with regard to the number of layers, activation functions, and so on). The selection of the model is done using the so-called NN model. Before making a final choice, it is common practise to calculate the performance achieved by some error metric when comparing the various model alternatives. This is done prior to making a decision. In order to accomplish this goal, the data from the previous two and a half years is divided into two distinct datasets. Figure 1 shows proposed model.

Additionally, available are the following three subsets of the model selection dataset shown in Figure 2:

- (i) Training Data: Readings of the irradiance over the course of at least one year are required for the purposes of training. This is done to prevent the CNN from becoming over fit to the data. This data split contains roughly half of the total model selection data
- (ii) Validation Data: Validation data is taken from irradiance measurements taken during a period of time

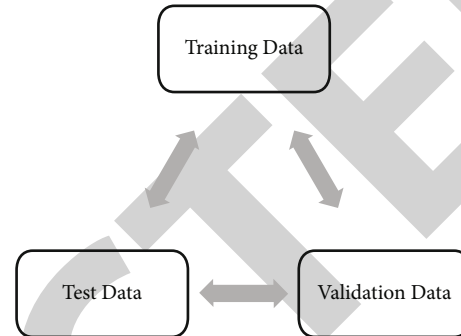


FIGURE 2: Subsets of the model selection dataset.

that is distinct from the training period and is also shorter. Re-evaluating this data at a variety of points throughout the training process allows for the determination of whether or not the CNN has become overfit. When something like this takes place, a strategy for early stop is put into play so that a general solution to the problem can be found. In the training data for this dataset, the length of the night is reduced. This data split contains a quarter of the total data for the model selection process. Training and Validation The reference data consist of irradiance values measured during the same time period as the test data. These values are used to train and validate models

- (iii) Test Data: The observations that had solar zenith angles that were greater than  $80^\circ$ , denoted by the notation  $s > 80^\circ$ , have been removed from this set. This is because of the low levels of irradiance that are present in the early morning and early evening hours, which is a time when the readings from a pyranometer are less accurate. This includes the nights because it is impossible to provide accurate forecasts for any topology during the night-time hours. This dataset, which represents the final 25% of the model selection data, is used to evaluate and compare the effectiveness of the various model architectures

**3.1. Non-Linear Model.** Systems are considered nonlinear if they do not conform to the superposition principle, which can only be achieved by being nonlinear. Numerous applications based on real-world data have demonstrated that nonlinear models, when compared to linear ones in nonlinear models, can produce more accurate predictions than the former. The NARMAX model is versatile enough to be

applied to the simulation of a wide variety of nonlinear systems. It has been demonstrated that NARMAX is capable of modelling a wide variety of systems that exist in the real world. The following equation provides a graphical depiction of the mathematical representation of the NARMAX model. The output of the model is affected in various ways by factors such as historical values, random noise, and outside input.

It is important to make a distinction between mild and severe nonlinearity when discussing nonlinear systems. Modelling of many different engineering systems can be accomplished with the help of stable, mildly nonlinear systems like NARX or NARMAX models. Real-world systems, such as those pertaining to the stock market, oil prices, meteorological systems, and hydrological systems, are receiving a growing amount of attention as a direct result of the widespread use of system identification technologies. There is a possibility that polynomial NARX and NARMAX models will not be able to make accurate predictions regarding these nonlinear, complex, and non-stationary systems.

#### 4. CNN for Prediction

The model that we will be using is a 13-layer convolutional neural network. The network is making use of LSTMs in order to model the function that transforms a H image of the Sun into a probability vector for each image containing a particular feature. If the features of an image are correctly learned by a neural network, then image classification can be made more accurate.

Between the input and the output of the system, the layers depicted in Figure 1 as cuboids are performing a significant number of large matrix computations. This process is repeated for each layer. The convolution kernels are made up of three 3x3 pixel squares, each of which was initially initialized by employing the HE initialization algorithm. To generate photovoltaic energy, it is necessary to capture photons of light held by solar radiation and convert it into electricity for use. This can be achieved through photovoltaic conversion process using solar panel. An important element of a solar panel is the photovoltaic cell. It is a semiconductor material (made of silicon) that requires no moving parts, no fuel, or noise. When this photovoltaic cell is continuously exposed to light, it absorbs the energy in the light's photons to generate energy, setting the electrons trapped by the internal electric field in motion. When this happens, the electrons collected on the surface of the photovoltaic cell generate a continuous current of electricity. In order for the network to learn which abstract features are being picked up by convolutions and which physical features they correspond to, it is the job of the optimizer to update the convolution kernel values while the network is being trained. A higher number of convolutions will be helpful in differentiating between these features.

The result of the convolution operation is then batch normalized after it has been processed. The equation provides a means of normalizing the convolution calculation relative to a batch mean ( $\beta$ ) and standard deviation ( $\gamma$ ).

The network reliability can be improved with the help of this method as in Equation (1).

$$y = \gamma \frac{x - E[x]}{\sqrt{\sigma(x) + \epsilon}} + \beta \quad (1)$$

where.

- x –output feature maps and.
- y – feature maps,
- $\epsilon$  - positive constant and.
- $\sigma$  –feature maps variance.

As a consequence of this, the dynamic range of the data is decreased, but the loss of two additional trainable parameters ( $\beta$ ,  $\gamma$ ) allows for the training process to be significantly sped up. It is possible to recover the true feature maps from the batch stabilized feature maps, as shown in Equation (1), if Equation (1) is manipulated while back-propagation is being performed. After the batch stabilization process is complete, the data is put through an activation function, which is a non-linear transformation. The output of the batch stabilization is shifted, and as a consequence, the signal that is being passed on to the subsequent layer has a different distribution. This particular function makes use of the rectified linear unit function as in equation (2).

$$\Phi(x) = \max(0, x). \quad (2)$$

This was chosen because of its ability to avoid gradient problem due to its sparse output. The reason for this ability is explained below. It is referred to as the vanishing gradient problem when the utilized gets stuck in the loss space due to decreasing gradients and back-propagation loss function gradients that are tending toward zero. It does not require extracting any static material to work. It produces very cheap energy, and its initial investment is easy to recover over several years. A major problem with renewable energy since its inception is the initial investment and its rate of return, although this is not thanks to the development of technology. A solar panel can have a useful life of 40 years. Using ReLUs allows one to circumvent this issue because the gradients of these models are invariably large as in Equation (3).

$$D\phi dx = H(x) \quad (3)$$

where.

$H(x)$ –Heaviside function.

Since this results in less spatial information, over-fitting is reduced. For the purpose of this downsampling, the image is sectioned off into  $2 \times 2$  grids of two-by-two-pixel segments so that the maximum amount of detail can be extracted from each individual segment. This indicates that in a down-sampled image, a single pixel represents the original four-pixel block that the image was taken from.

Because each pixel in the input image represents more information from the original input, the network is able to learn more complex features by performing operations on a larger fraction of the original image (for example, four

pixels instead of one), which highlights larger, more complex features via the convolution operation. This allows the network to learn more complex features more quickly. It is possible to reduce over-fitting by 12tilized12 other methods such as average pooling, but maxpooling is the most widely used method because of the benefits it provides in reducing over-fitting. Other methods includes the fully-connected block and dropout 12tilized12ed12on are two of the most important concepts to understand in relation to this network. If there are  $N$  input nodes and  $M$  output nodes, then a linear transformation will result in  $N \times M$  parameters that need to be changed for a layer to have a fully-connected topology. Dropout is a more recent development in the field of machine learning. In order for the network to train on an approximation of the actual structure of the network, it gives every node and connection an equal probability of being ignored while it is in the training phase. At the time of validation, an effective 12tilized12ed12on technique that reduces over-fitting while maintaining accuracy is to train the data set. The third fully-connected layer is what determines the classification of the images. In our model, the class labels are inferred based on the loss function that we choose to use, which also implicitly adds this last layer of activation.

**4.1. Training.** The training phase of a machine learning algorithm is by far the most difficult and significant part of the overall process. Training is the process by which a network learns which algorithm it should be approximating in order to achieve optimal performance. For the purpose of implementing this in the network, a feed-forward and back-propagation system are used. The number of epochs (full passes) of the feed-forward and back-propagation algorithm is another hyper-parameter, which means it is a parameter that the system does not learn and that needs to be tuned during training.

The images are being fed from input to output through the network, which is referred to as the network having a feed-forward nature. The way a NN is initially trained can have a significant effect on how well it performs. We use something that is known as He initialization rather than random or zero initialization of the weights because this allows us to reduce the number of epochs that are necessary for learning. Here, weights are selected at random from the normal distribution  $N(0, \sigma)$ , and the resulting matrix is 13utilized13ed as follows in Equation (4):

$$\sigma = \sqrt{\frac{2}{n_l}} \quad (4)$$

where.

$n_l$  – total connections across layer  $l$ .

In order to obtain this result, the variance of the forward linear process of the neural network was 13tilized. First, as a result of this initialization, a machine learning algorithm was able to classify images more accurately than a human could.

To determine which category an image falls under, the network consults the weights it has been trained with after the feed-forward process is complete. After that, the process

of back-propagation starts, in which each weight in the network gets updated so that the number of incorrect classifications gets lower the next time this process starts. This completely clean energy helps reduce your carbon footprint significantly. Thanks to its use we avoid the generation of greenhouse gases and we do not pollute either in its generation or in its use. There is very little pollution involved in the manufacturing of solar panels. Back-propagation optimization employs a technique known as stochastic gradient descent (SGD). The network perception of reality is compared to that perception using a function called the loss function, which measures the difference. Using a first-order gradient method, which is very simple to calculate mathematically, the weights can be easily and quickly updated as in Equation (5).

$$\Theta_{t+1} = \theta_t + \eta \nabla_{\theta} L(x; \theta_t) \quad (5)$$

where.

$\theta_{t+1}$  – updated weight.

$\eta$  – learning rate.

The learning rate refers to the process of calculating how much of a change in weight will take place in the loss space of the loss function. This hyper-parameter, which is the second of two that will be tested throughout the training, will also be examined. This method is very similar to standard SGD, but it also includes a velocity term that causes weight updates to accelerate over the course of multiple epochs. This velocity can then be added as follows as in Equation (6):

$$\theta_{t+1} = \theta_t + v_{t+1} = \theta_t + \mu v_t - \eta \nabla_{\theta} L(x; \theta_t + \mu v_t) \quad (6)$$

When the gradient is updated, the product of the momentum coefficient ( $\mu$ ) and the velocity ( $v_t$ ) is also updated. This means that  $\theta_{t+1}$  is not only updated by the gradient; it is also updated by the product of  $\mu$  and  $v_t$ . When predictions are not accurate as a result of an argument in the gradient gradient argument, this feature enables a faster correction of the velocity term. If the product  $\mu v_t$  leads to inadequate weight updates, the optimizer may wish to try again in a different direction. Gradient functions have a tendency to become steeper when there are insufficient updates to the weights. With SGD and Nesterov momentum, we will not overshoot the target because the regions with flatter curvature are located closer to the minima. Because of this, we are able to move through the lost space at a faster rate.

Altering the values of the two other hyper-parameters enables a set of models to be trained. In order to reach general convergence, various problems require significantly varying numbers of epochs. The results cannot be reliable if there are not enough epochs because the model will be underfit if there are not enough of them. Overfitting can happen when the number of epochs is too high, and when this happens, the network may incorrectly classify data that it has never encountered before. Determining the optimal number of epochs is one way to avoid underfitting. However, overfitting should also be avoided at all costs. In addition, some of the training data can be used in the phase of validation rather than in the phase of training. Because of

this, for instance, it will be possible to monitor how the network reacts to unknown data because the validation data will have a predetermined category. However, the converse is also possible: the system may never get out of a bad local minimum, which will cause it to arrive at a solution that is suboptimal.

## 5. Results and Discussions

The performance of the suggested CNN models is evaluated with the help of a pyranometer for two different reasons. The selection of a model is the first step in determining the optimal structure that should be applied. The definitive findings will be reported once the model has been evaluated. In addition to this, the study investigates and quantifies the extent to which the accuracy of a forecast can be improved by the addition of additional datasets during the stage where the model is being evaluated. The results are 99.92% accurate with optimal hyper-parameters at the rate of  $\eta=5 \times 10^{-4}$ , which we determined by training and validating across the hyper parameter ranges.

It is possible to draw the conclusion that our model has not successfully encapsulated all of the possible input-output mapping functions. Because it is difficult to find an image data classifier that is free of distortions and artefacts, which can cause misclassification, one should not underestimate how close this model comes to being perfect. Only discrete steps have been taken by us in the hyper-parameter space, which may result in a classification that is even more accurate.

Our model is contrasted with the persistence model, which acts as a benchmark for comparing other models to. This model is used because it is predicated on the assumption that there will be no change in the amount of radiation over the course of the forecast period. In addition to being called the root mean square error (RMSE), the mean absolute error is another name for it. In addition to this, it is used to determine the degree to which the forecasting model is an improvement on the reference persistence model. It is not possible to deduce from the classification percentage of a validation set whether or not our classifier has learned what we wanted it to base on the available statistical evidence. This can be caused by an uneven split in the validation set as well as by a classification task that has a strong bias. To solve this problem, our classifier makes use of something called a confusion matrix. In contrast to the classification determined by the network, the actual class of an image is reflected in this matrix.

Each class would have an equal amount of precision and recall. A deviation from one in the precision is produced whenever the instances is incorrectly classified. Every other class has a precision of one, which indicates that the network does not consider any images that do not contain these features to actually contain them even if they appear in the image. The only one of the recalls that is different from the others is an image that has an incorrect classification. This means that the network will never attribute a feature to any of those images that is not actually present in the image itself. This applies to each and every one of those images.

TABLE 1: Accuracy of Prediction.

| Training samples | CNN      | RCNN     | U-net    | Proposed |
|------------------|----------|----------|----------|----------|
| 100              | 91.90767 | 92.44058 | 93.29245 | 94.16016 |
| 200              | 90.55034 | 91.07538 | 91.91467 | 92.76957 |
| 300              | 92.29715 | 92.83231 | 93.68779 | 94.55919 |
| 400              | 88.77206 | 89.28679 | 90.10959 | 90.94771 |
| 500              | 91.52316 | 92.05383 | 92.90214 | 93.76623 |
| 600              | 92.14522 | 92.67951 | 93.53358 | 94.40354 |
| 700              | 92.11339 | 92.64749 | 93.50127 | 94.37093 |
| 800              | 90.25394 | 90.77726 | 91.6138  | 92.4659  |
| 900              | 92.83424 | 93.37252 | 94.23298 | 95.10944 |
| 1000             | 90.4031  | 90.92728 | 91.76521 | 92.61872 |

TABLE 2: Precision.

| Training samples | CNN      | RCNN     | U-net    | Proposed |
|------------------|----------|----------|----------|----------|
| 100              | 92.14559 | 92.67988 | 93.53396 | 94.40392 |
| 200              | 88.57739 | 89.09098 | 89.91199 | 90.74826 |
| 300              | 91.33169 | 91.86125 | 92.70778 | 93.57006 |
| 400              | 92.03151 | 92.56514 | 93.41815 | 94.28704 |
| 500              | 90.85801 | 91.38483 | 92.22697 | 93.08478 |
| 600              | 90.09833 | 90.62075 | 91.45585 | 92.30648 |
| 700              | 92.39287 | 92.9286  | 93.78496 | 94.65726 |
| 800              | 85.82268 | 86.3203  | 87.11577 | 87.92604 |
| 900              | 89.81567 | 90.33645 | 91.16893 | 92.01689 |
| 1000             | 92.16017 | 92.69454 | 93.54875 | 94.41885 |

The misunderstanding of our network does not bring about any detrimental effects to its functioning. Due to the fact that the margin of error is very small, we are confident that our network has learned the geometry of these features. It is essential to carry out both analyses because, if the deterioration in the forecast is deemed tolerable, there will be a reduction in the amount of money needed to implement the forecasting model. It is not necessary to leave a temporary pyranometer at the location of the target because a portable pyranometer can be used to collect training data and then moved to a different location.

Tables 1–4 demonstrates that, as was to be expected, the rRMSE obtained from real-world measurements is noticeably lower than that which was obtained through simulations. Nevertheless, there are a variety of other outcomes that could occur. Real-time irradiance feedback is of comparable or even slightly greater significance for the shorter-term predictions than it is for the longer-term forecast. However, it is important to note that forecasts that are not based on any actual data can still be useful in many different contexts. For time horizons of more than 30 minutes, all other models have a performance advantage over the persistent model. In point of fact, as the horizon gets higher, the influence of actual measurements on the quality of the forecast becomes less significant, while the advantage of using a clear-sky model grows. In conclusion, it can be observed

TABLE 3: Recall.

| Training samples | CNN      | RCNN     | U-net    | Proposed |
|------------------|----------|----------|----------|----------|
| 100              | 92.60026 | 93.13718 | 93.99547 | 94.86973 |
| 200              | 90.52414 | 91.04903 | 91.88807 | 92.74273 |
| 300              | 90.47007 | 90.99464 | 91.83318 | 92.68733 |
| 400              | 92.14522 | 92.67951 | 93.53358 | 94.40354 |
| 500              | 88.19033 | 88.70169 | 89.5191  | 90.35172 |
| 600              | 88.54223 | 89.05562 | 89.8763  | 90.71224 |
| 700              | 92.02507 | 92.55866 | 93.41161 | 94.28044 |
| 800              | 90.64418 | 91.16976 | 92.00992 | 92.8657  |
| 900              | 88.34328 | 88.85552 | 89.67436 | 90.50842 |
| 1000             | 92.30929 | 92.84453 | 93.70012 | 94.57163 |

TABLE 4: F-measure.

| Training samples | CNN      | RCNN     | U-net    | Proposed |
|------------------|----------|----------|----------|----------|
| 100              | 92.14559 | 92.67988 | 93.53396 | 94.40392 |
| 200              | 88.18804 | 88.69938 | 89.51677 | 90.34937 |
| 300              | 90.2786  | 90.80206 | 91.63883 | 92.49116 |
| 400              | 92.37265 | 92.90825 | 93.76443 | 94.63654 |
| 500              | 91.79955 | 92.33183 | 93.18269 | 94.04939 |
| 600              | 90.87638 | 91.40331 | 92.24562 | 93.1036  |
| 700              | 92.09863 | 92.63264 | 93.48628 | 94.3558  |
| 800              | 88.4745  | 88.9875  | 89.80755 | 90.64285 |
| 900              | 90.25739 | 90.78073 | 91.6173  | 92.46943 |
| 1000             | 91.86191 | 92.39456 | 93.246   | 94.11328 |

how the skill of the forecast begins to decrease with longer horizons, which exemplifies a limitation of satellite-based forecasts that is already well known.

## 6. Conclusions

Utilizing the DNN that was developed for the purpose of this study could make intraday forecasting of solar irradiance more accurate, thereby improving the controllability of power plants. The accuracy of the model has also been evaluated in light of the data sources that are at our disposal. In general, four different cases have been investigated. The DNN forecasting system uses a irradiance forecast for the future as a starting point. However, actual data from the target location can only be gathered during the training phase of the DNN. This data can only be used as a form of feedback to the forecasting system. According to the findings, the DNN is capable of making accurate predictions regarding solar radiation and, in every scenario, it outperforms the persistent algorithm. Even if there are no real-world observations available, the results of the proposed model outperform those of the current NWP forecasts for the same time horizon as the NWP forecasts. When making predictions for the short term, using actual data to reduce the margin of error can be helpful. When making predic-

tions for the long term, however, weather information can be beneficial.

## Data Availability

The data used to support the findings of this study are included within the article. Further data or information is available from the corresponding author upon request.

## Conflicts of Interest

The authors declare that there is no conflict of interest regarding the publication of this article.

## Funding

This research work is not funded from any organization.

## Acknowledgments

The authors appreciate the supports from University of Gondar, Ethiopia. for providing help during the research and preparation of the manuscript.

## References

- [1] K. K. R. Samal, K. S. Babu, and S. K. Das, "Multi-directional temporal convolutional artificial neural network for PM2.5 forecasting with missing values: A deep learning approach," *Urban Climate*, vol. 36, article 100800, 2021.
- [2] M. Shen, H. Zhang, Y. Cao, F. Yang, and Y. Wen, "Missing data imputation for solar yield prediction using temporal multi-modal Variational auto-encoder," in *Proceedings of the 29th ACM International Conference on Multimedia*, pp. 2558–2566, New York, 2021.
- [3] H. Sun, K. J. Kuchenbecker, and G. Martius, "A soft thumb-sized vision-based sensor with accurate all-round force perception," *Nature Machine Intelligence*, vol. 4, no. 2, pp. 135–145, 2022.
- [4] W. Li, Z. Shang, S. Qian, B. Zhang, J. Zhang, and M. Gao, "A novel intelligent fault diagnosis method of rotating machinery based on signal-to-image mapping and deep Gabor convolutional adaptive pooling network," *Expert Systems with Applications*, vol. 205, p. 117716, 2022.
- [5] K. Yadav, M. Yadav, and S. Saini, "Stock values predictions using deep learning based hybrid models," *CAAI Transactions on Intelligence Technology*, vol. 7, no. 1, pp. 107–116, 2022.
- [6] Y. Shen, Y. Ma, S. Deng, C. J. Huang, and P. H. Kuo, "An ensemble model based on deep learning and data preprocessing for short-term electrical load forecasting," *Sustainability*, vol. 13, no. 4, p. 1694, 2021.
- [7] Y. Qian, Z. Huang, H. Fang, and Z. Zuo, "WGLFNets: Wavelet-based global-local filtering networks for image denoising with structure preservation," *Optik*, vol. 261, article 169089, 2022.
- [8] X. J. Sun and J. C. W. Lin, "A target recognition algorithm of multi-source remote sensing image based on visual internet of things," *Mobile Networks and Applications*, vol. 27, no. 2, pp. 784–793, 2022.
- [9] Y. Yuan, K. Dehghanpour, Z. Wang, and F. Bu, "A joint distribution system state estimation framework via deep actor-critic

- learning method,” *IEEE Transactions on Power Systems*, vol. 2022, 2022.
- [10] C. Yang, Y. He, C. Sun, S. Jiang, Y. Li, and P. Zhao, “Infrared and visible image fusion based on QNSCT and guided filter,” *Optik*, vol. 253, article 168592, 2022.
- [11] C. Cai, Z. Guo, B. Zhang, X. Wang, B. Li, and P. Tang, “Urban morphological feature extraction and multi-dimensional similarity analysis based on deep learning approaches,” *Sustainability*, vol. 13, no. 12, p. 6859, 2021.
- [12] R. Dhinakaran, R. Muraliraja, R. Elansezhian, S. Baskar, S. Satish, and V. S. Shaisundaram, “Utilization of solar resource using phase change material assisted solar water heater and the influence of nano filler,” *Materials Today: Proceedings*, vol. 37, pp. 1281–1285, 2021.
- [13] Y. D. Borole, J. Dofe, and C. G. Dethé, “Machine Learning-Enabled Techniques for Reducing Energy Consumption of IoT Devices,” in *Green Internet of Things and Machine Learning: Towards a Smart Sustainable World*, pp. 27–85, Wiley, 2021.
- [14] A. Jayashree, V. Kudva, and A. G. Ananth, “Microcontroller-Based Control Circuit for the Automatic Orientation of Solar Panels in the Direction of Sun,” in *Advances in VLSI, Signal Processing, Power Electronics, IoT, Communication and Embedded Systems*, pp. 289–302, Springer, Singapore, 2021.
- [15] M. Wang, C. Sun, and A. Sowmya, “Complex shearlets and rotary phase congruence tensor for corner detection,” *Pattern Recognition*, vol. 128, article 108606, 2022.
- [16] H. Liu, J. Qiao, L. Li, L. Wang, H. Chu, and Q. Wang, “Parallel CNN Network Learning-Based Video Object Recognition for UAV Ground Detection,” *Wireless Communications and Mobile Computing*, vol. 2022, Article ID 2701217, 19 pages, 2022.
- [17] Z. Qin, Q. Zeng, Y. Zong, and F. Xu, “Image inpainting based on deep learning: a review,” *Displays*, vol. 69, article 102028, 2021.
- [18] J. Fan, Q. Hua, X. Li, Z. Wen, and M. Yang, “Biomedical sensor image segmentation algorithm based on improved fully convolutional network,” *Measurement*, vol. 197, article 111307, 2022.
- [19] Y. Yang and J. Chen, “Comprehensive analysis of water carrying capacity based on wireless sensor network and image texture of feature extraction,” *Alexandria Engineering Journal*, vol. 61, no. 4, pp. 2877–2886, 2022.
- [20] A. K. Bashir, S. Khan, B. Prabadevi et al., “Comparative analysis of machine learning algorithms for prediction of smart grid stability,” *International Transactions on Electrical Energy Systems*, vol. 31, no. 9, article e12706, 2021.
- [21] L. B. Cross, R. A. S. I. Subad, M. M. H. Saikot, and K. Park, “Waterproof Design of Soft Multi-Directional Force Sensor for underwater robotic applications,” *Applied Mechanics*, vol. 3, no. 3, pp. 705–723, 2022.
- [22] X. Zhu, R. Wang, Z. Fan, D. Xia, Z. Liu, and Z. Li, “Gearbox fault identification based on lightweight multivariate multidirectional induction network,” *Measurement*, vol. 193, article 110977, 2022.
- [23] Z. Chen, C. Wang, J. Li, B. Zhong, J. Du, and W. Fan, “Combined improved Dirichlet models and deep learning models for road extraction from remote sensing images,” *Canadian Journal of Remote Sensing*, vol. 47, no. 3, pp. 465–484, 2021.
- [24] A. D. Patange and R. Jegadeeshwaran, “Review on tool condition classification in milling: a machine learning approach,” *Materials Today: Proceedings*, vol. 46, pp. 1106–1115, 2021.
- [25] H. A. Amirkolaei, H. Arefi, M. Ahmadlou, and V. Raikwar, “DTM extraction from DSM using a multi-scale DTM fusion strategy based on deep learning,” *Remote Sensing of Environment*, vol. 274, article 113014, 2022.
- [26] H. Luo and W. Zhao, “Multi-focus image fusion through pixel-wise voting and morphology,” *Multimedia Tools and Applications*, vol. 2022, pp. 1–27, 2022.
- [27] N. Iqbal, F. Jamil, S. Ahmad, and D. Kim, “A novel blockchain-based integrity and reliable veterinary clinic information management system using predictive analytics for provisioning of quality health services,” *IEEE Access*, vol. 9, pp. 8069–8098, 2021.
- [28] Y. Pan, D. Liu, L. Wang, J. A. Benediktsson, and S. Xing, “A Pan-sharpening method with Beta-divergence non-negative matrix factorization in non-subsampled shear transform domain,” *Remote Sensing*, vol. 14, no. 12, p. 2921, 2022.
- [29] Y. Xu and Z. Wang, “Visual sensing technologies in robotic welding: recent research developments and future interests,” *Sensors and Actuators A: Physical*, vol. 320, article 112551, 2021.